Sustainable Food Technology

ROYAL SOCIETY OF CHEMISTRY

PAPER

View Article Online
View Journal | View Issue

Check for updates

Cite this: *Sustainable Food Technol.*, 2024, **2**, 1697

Utilization of tamarind kernel powder for the development of bioplastic films: production and characterization

Rokalla Preethi,[ab] Amrutha N. R.,[ab] P. S. Keshava Murthy[ab] and Jeevan Prasad Reddy *[ab]

Received 28th June 2024
Accepted 29th August 2024

DOI: 10.1039/d4fb00199k

rsc.li/susfoodtech

Global plastic production is on a rapid and alarming rise, posing a significant threat to our environment due to plastic's non-biodegradable nature. In response to this urgent issue, the present study aimed to develop eco-friendly plastic films from tamarind kernel powder (TKP) and PBAT using melt blending, followed by cast-film extrusion. Tamarind kernel powder was subjected to proximate and physico-chemical analysis. The effect of the TKP content (10, 20, and 30 wt%) and plasticizers (glycerol and polyethylene glycol) on the blending of PBAT was investigated. These bioplastic films were subjected to compatibility, mechanical, thermal, water barrier, UV-vis spectroscopy, and overall migration and biodegradation studies. From proximate analysis, the major constituent of TKP powder was found to be xyloglucan, accounting for 66.8% of the total carbohydrates. FTIR analysis showed that TKP has strong interactions with PBAT. SEM micrographs revealed that 30% of the TKP films had an increased roughness and uniform dispersion, which was found in the presence of plasticizers. UV-visible spectroscopy analysis showed that transmittance decreased with an increase in the concentration of TKP. The tensile strength of TKP inclusion films decreased with an increase in concentration, whereas their modulus enhanced, showing increased film stiffness. Overall, migration studies showed that TKP inclusion films had higher migration than neat PBAT films owing to the top hydrophilic nature of TKP powder.

Open Access Article. Published on 18 settembre 2024. Downloaded on 05/04/2026 03:54:11.
This article is licensed under a Creative Commons Attribution-NonCommercial 3.0 Unported Licence.

Sustainability spotlight

Tamarind kernel powder (TKP) is a natural polysaccharide obtained from tamarind seeds. TKP is nontoxic and safe for food contact applications, making it suitable for use in food packaging. After disposal, TKP films, being biodegradable, can breakdown into natural compounds through the action of microorganisms, contributing to reduced environmental impact compared to conventional plastics. TKP does not leach harmful chemicals into the environment or food products. TKP can be used in combination with biodegradable polymers to create flexible packaging films with desirable properties that would be suitable for food packaging, agricultural films, and compostable bags. Additionally, the biodegradability of TKP films reduces the accumulation of plastic waste in landfills and oceans. Overall, owing to their biodegradability, byproduct utilization, safety, and versatility, tamarind kernel powder packaging films are an attractive option for sustainable packaging solutions.

1 Introduction

Recently, the development of packaging materials from natural resources has increased rapidly because of the hazardous effects of non-biodegradable conventional plastics (polyethylene terephthalate (PET), polystyrene (PS), polyethylene (PE) and polypropylene (PP)), which affect the environment and result in serious human health problems. Safety concerns associated with conventional plastics are increasing, which has driven the increasing demand for biodegradable plastic-based packaging.[1] Thus, biodegradable polymers have become a practical substitute for non-biodegradable plastics in many industrial applications. The global market for biodegradable plastic packaging was estimated to be worth around USD 4.65 billion in 2019. By the end of 2025, it is projected to have grown at a compound annual growth rate (CAGR) of 17.04%, with a potential market value of USD 12.06 billion. Polybutylene succinate (PBS), poly(butylene adipate-*co*-terephthalate) (PBAT), starch blends, polylactic acid (PLA), polyhydroxyalkanoates (PHA), and other biodegradable polymers account for more than 55.5% of the world's total production of bioplastics.[2] With growing environmental concerns, many government organizations are developing stringent rules to avoid the use of single-use plastics. Numerous industries employ bioplastics, including consumer electronics, automotive, building and construction, horticulture and agriculture, coatings, and rigid

[a]*Polymer Materials Lab, Food Packaging Technology Department, CSIR-Central Food Technological Research Institute, Mysuru 570020, India. E-mail: jreddy@cftri.res.in*
[b]*Academy of Scientific and Innovative Research (AcSIR), Ghaziabad, Uttar Pradesh 201002, India*

© 2024 The Author(s). Published by the Royal Society of Chemistry

Open Access Article. Published on 18 settembre 2024. Downloaded on 05/04/2026 03:54:11.
This article is licensed under a Creative Commons Attribution-NonCommercial 3.0 Unported Licence.

and flexible packaging. Packaging is a predominant application, accounting for almost 53% (1.14 million tons) of the total bioplastics produced in 2019.[3]

Biodegradable packaging is prepared from bio-based materials capable of undergoing decomposition into carbon dioxide, methane, water, inorganic compounds, or biomass, predominantly by the enzymatic action of microorganisms.[4,5] Biodegradable films have been developed from naturally derived molecules such as polysaccharides, proteins, and lipids, which can be obtained from agro and food byproducts.[6] Food processing industries produce a substantial amount of agricultural waste each year, with seeds, kernels, leaves, stems, and roots being some of the possible sources. Polysaccharides are widely available and are among the most affordable biodegradable polymers. Many biodegradable materials, such as polysaccharide-based materials, are hydrophilic and highly crystalline, negatively influencing their performance and processing. For this reason, the structure of these bio-based packaging materials must be modified to give them thermoplastic properties.[5] Among all the agricultural byproducts, tamarind kernel powder (TKP) is one of the most polysaccharide-rich components, made from the seeds of *Tamarindus indica* Linn, a member of the Leguminosae family. TKP is mainly composed of side chains of α-D-xylopyranose (1→4) and β-D-glucopyranosyl (1→2), as well as β-D-glucan-α-D-xylopyranose.[7]

The monosaccharide units in TKP, such as xylose, glucose, and galactose, have a molar ratio of 2.25 : 2.8 : 1.0.[8] India produces 0.3 million tons of tamarind annually. The specific qualities of TKP, including its good stability at acidic pH, quick biodegradability, biocompatibility, and nontoxic nature, are attributed to its proximal composition.[7] As per the FDA, tamarind kernel powder can be safely used for articles intended for manufacturing, processing, packaging, and transporting applications. It has excellent film-forming capability. For instance, chitosan–tamarind seed polysaccharide,[9] carboxymethyl tamarind gum-polyvinyl alcohol,[10] and tamarind kernel xyloglucan and sesame seed oil[11] have all been used to develop composite films. However, TKP-based polysaccharides possess poor barrier, mechanical, and thermal properties, which limit their ability to meet the desired requirements for food packaging uses. These limitations include their bad odor, poor color, availability of water-insoluble particles, and lower solubility in cold water.[12] Therefore, modifications are also required to enhance the functionality and physicochemical characteristics of the films, such as higher water vapor barrier and moisture resistance properties and adequate mechanical and optical properties by impregnating TKP with some bioplastics.[5]

Some common bioplastics include polyhydroxyalkanoate (PHA), polylactic acid (PLA), poly(butylene-succinate) (PBS), and poly (butylene adipate co-terephthalate) (PBAT). Among them, PBAT has drawn much attention as a possible replacement for low-density polyethylene. It is a linear aromatic co-polyester produced by the condensation of 1,4-butanediol, terephthalic acid, and adipic acid.[11] This could be the best choice for a packaging material because of its biocompatibility, high flexibility, good processability, and high tear resistance, which make it suitable for use in the food packaging sector.[12–14] Furthermore, it exhibits short molding cycles and superior sealing capabilities, and it is facile to handle at elevated extrusion speeds.[15,16] However, the widespread application of PBAT in packaging materials is limited due to its cost compared to typical conventional plastics. A potential way to improve the effectiveness of PBAT-based plastic is to blend plasticized materials, like starch, at 20–30 wt% of the total weight of the polymer.[17] Surprisingly, we could find no studies on tamarind kernel powder with PBAT for packaging applications. However, weak interfacial adhesion between the two phases results from the noticeable differences in their solubility parameters due to the hydrophilic nature of TKP and hydrophobic nature of PBAT. Adding plasticizers like glycerol, sorbitol, or polyethylene glycol could address this problem. Plasticizers are low molecular weight compounds that reduce the temperature of glass transition materials used for film-forming. Plasticizers make the film more flexible, robust, and tear-resistant, decrease the brittleness, and improve the material's elasticity.[5,18] Among these additives, glycerol has been chiefly used to produce many starch-based films because of its low cost and compatibility, stimulating better mechanical properties by interfering with the molecules. Polyethylene glycol (PEG) is another of the most used plasticizers. It is a water-soluble polyether that is nontoxic, biocompatible, and biodegradable.

This work blended TKP with PBAT at different weight ratios and in the presence of plasticizers using a solvent-free melt blending method. We investigated the influence of TKP and plasticizers on the mechanical, thermal properties, UV barrier, morphology, and degradability of PBAT blends. This study highlights how the TKP ratio strongly affects the characteristics of different TKP/PBAT blends.

2 Experimental section

2.1. Materials

Raw materials, including tamarind kernel powder, an industrial by-product, were procured from Hindupur in Andhra Pradesh, while PBAT was obtained from Ecoworld® 003 (Jinhui Zhaolong High Technology Co., Ltd) with a density of 1.26 kg m^{-3}. Glycerol (purity of 99.5%), polyethylene glycol, 2,2-diphenyl-1-picrylhydrazyl, methanol, and chloroform were obtained from Sigma-Aldrich.

2.2. Methods

2.2.1. Physicochemical aspects of tamarind kernel powder. The chemical composition (moisture content, crude protein, crude fat, total ash, crude fiber, xyloglucan, total carbohydrates) was determined using an AOAC 2000 system.[19] All the proximate results were expressed as a percentage of the weight of the sample analyzed. The physical properties, including pH, viscosity, water absorption index (WAI), water solubility index (WSI), bulk density, tap density, Hausner ratio, compressibility index, and angle of repose, were also determined.

2.2.2. Compounding and production of films. Polymer compounding is a process in which various additives and materials are mixed with a base polymer to achieve a uniform

© 2024 The Author(s). Published by the Royal Society of Chemistry

Open Access Article. Published on 18 settembre 2024. Downloaded on 05/04/2026 03:54:11.
This article is licensed under a Creative Commons Attribution-NonCommercial 3.0 Unported Licence.

dispersion and tailor the properties of the final polymer compound. Compounding the TKP/PBAT blends was performed using a twin-screw extruder with a pelletizer and an attached air-cooling system to solidify the blends. Before compounding, PBAT and tamarind kernel powder were dried in a hot air oven to attain a moisture content of 2%. After drying, these materials were mixed in varying proportions of PBAT : TKP of 9 : 1, 8 : 2, and 7 : 3, and blends were developed. Beyond these ratios, voids were visually observed, and the blends turned powdery due to the immiscibility of the two polymers. Hence, plasticizers like glycerol and PEG were added at a 5% to 7 : 3 blend ratio to improve their compatibility. The processing parameters, such as screw speed (80–100 rpm), temperature (120–150 °C), and feeder speed (5–8 rpm), were adjusted. Later, the blends were subjected to cast-film extrusion with varying the temperature (115–135 °C) and screw speed (4–6 rpm). These prepared films were collected and stored in airtight pouches for further characterization (Table 1).

2.3. Characterization

2.3.1. Melt flow index. Several material characteristics, including the processing behavior, long-term viscoelastic behavior, and stability throughout end usage, can be predicted based on the melt flow rate. Therefore, it is a significant quality control factor for various polymeric materials. The weight of the polymer in grams that flows through a die with a specific diameter and length in 10 min when pressurized from a particular weight at a given temperature is called the melt flow index (MFI), where MFI = the weight of the sample in grams/10 min. The test was done at 190 °C, with a 2.16 kg load using a melt flow rate tester (CEAST model 7026.000) as per ASTM D1238-2023.[20]

2.3.2. Thickness of the films. The film's thickness was measured using a screw gauge. The tensile strength was calculated using the mean of the triplicates measured at random points throughout the length of the strip.

2.3.3. Tensile properties. The tensile properties were studied using a LLOYDS universal testing machine (LLOYDA-50k, London, UK) to measure the mechanical properties. According to the ASTM D-882 (ref. 21) standard test, the tensile strength (TS, MPa), Young's modulus (E, MPa), and elongation at break (ε, %) were measured. The samples were tested at a crosshead speed of 50 mm min^{-1}. The mechanical parameters reported are average values calculated from six measurements.

2.3.4. Moisture content. Every film sample was cut into 2 × 2 cm and placed in a Petri dish. The samples were dried at 75 °C in an oven for one day. The weight loss was obtained by calculating (eqn (1)) the percentage before and after drying and is reported as a change in water content based on the initial weight of the film.

$$\text{Moisture } (\%) = \frac{(W_1 - W_2)}{W_1} \times 100 \quad (1)$$

where W_1 is the initial weight of the film, and W_2 is the final weight of the film.

2.3.5. Water vapor transmission rate. Water vapor transmission rate (WVTR) testing was performed to determine the film's ability to prevent water vapor from passing through the film in a controlled environment. Using the standard ASTM E-96 technique[22] at 90% relative humidity and 38 °C, the film's WVTR was determined. The films were cut into an area measuring 9 cm in diameter. The aluminum cups used for the test were filled with 10 mL of distilled water, and the films were sealed on top of the cups using hot wax. The cups were then weighed, and the readings were noted. The weight of the aluminum cup was recorded after every day, and the test was concluded after eight days. The recording difference between the initial weight and final weight of the cups determined the weight loss caused by water evaporation through the films. The weight loss was plotted *versus* time, and the WVTR was calculated using the formula below (eqn (2)) below by a linear least-square approach.

$$\text{WVTR} = \frac{\text{slope}}{\text{area of the film}} \left(\text{g per m}^2 \text{ per day}\right) \quad (2)$$

where slope $= \frac{\Delta m}{\Delta t}$, where Δm is the mass change, and Δt is the time.

2.3.6. Water absorption index. Water absorption was determined following ASTM D570,[23] whereby the film samples were first dried in an oven for a predetermined time and temperature and then placed in a desiccator to cool. Immediately upon cooling, the specimens were weighed (W_1). These films were then soaked in water at 23 °C for an hour or until they attained equilibrium. The weight was again recorded (W_2) after removing the films and patting them dry with a lint-free cloth. The weight percentage increase was used to express the water absorption using eqn (3).

$$\text{Water absorption } (\%) = \frac{W_2 - W_1}{W_1} \times 100 \quad (3)$$

2.3.7. Water solubility index. The film samples were cut into a 2 × 2 cm strip to estimate the water solubility index. After drying, the films were weighed (W_1) and placed in distilled water. The undissolved films were then dried at 80 °C till they attained a uniform weight (W_2), which was used to calculate (eqn (4)) the final weight of the dehydrated insoluble film.

$$\text{Water solubility } (\%) = \frac{W_1 - W_2}{W_1} \times 100 \quad (4)$$

2.3.8. Morphology. The films' morphology was studied by scanning electron microscopy (SEM) (S-3700, Hitachi, Japan). A

Table 1 Composition of the tested PBAT-TKP blends

Films	PBAT (%)	TKP (%)	Glycerol (wt%)	PEG (wt%)
PT	100	—	—	—
PT10	90	10	—	—
PT20	80	20	—	—
PT30	70	30	—	—
PTG	70	30	5	—
PTP	70	30	—	5

© 2024 The Author(s). Published by the Royal Society of Chemistry

Open Access Article. Published on 18 settembre 2024. Downloaded on 05/04/2026 03:54:11.
This article is licensed under a Creative Commons Attribution-NonCommercial 3.0 Unported Licence.

Table 2 Proximate and physical properties of TKP[a]

Proximate parameters	Results (%)	Physical properties	Results
Moisture	6.00 ± 0.35	pH	7.5 ± 0.42
Crude protein	18.7 ± 1.20	Viscosity (centipoise)	512 ± 1.35
Crude fat	6.00 ± 0.25	Bulk density (g cm^3)	0.38 ± 1.24
Total ash	3.79 ± 0.80	Tap density (g cm^3)	0.625 ± 1.62
Crude fiber	0.49 ± 2.15	Hausner ratio	1.625 ± 1.30
Carbohydrates	71.14 ± 1.80	Compressibility index (%)	28.15 ± 0.60
Xyloglucan	66.8 ± 0.75	Angle of repose (degree)	34.85 ± 1.24
Energy (kcal per 100 g)	368	Water absorption index (%)	415.37 ± 1.15
		Water solubility index (%)	38.78 ± 1.42

[a] Mean ± SD of triplicates.

Table 3 Melt flow index[a]

Films	Melt flow index (g per 10 min)
PT	17.840 ± 0.036^e
PT10	12.236 ± 0.035^d
PT20	11.750 ± 0.040^c
PT30	10.240 ± 0.029^b
PTG	7.090 ± 0.020^a
PTP	17.840 ± 0.036^e

[a] Each value is the standard deviation + the mean of the triplicates. According to Duncan's multiple range test, any two means in the same column that are separated by the same superscript letter were not substantially ($p > 0.05$) different.

layer of gold was sputter coated onto the samples. The surface of PBAT and its biocomposite films was tested at 10 kV resolution.

2.3.9. Antioxidant property. The free radical scavenging assay was used to assess the PBAT/TKP film's capacity to scavenge free radicals. Methanol was used as a reference in this study. Here, 50 mg of the film was added in 10 mL of DPPH methanol solution (1 mM). This solution was agitated for 5 min and kept in the dark at room temperature for 30 min. The absorbance was then measured at 517 nm. Using the following formula (eqn (5)), the percentage free radical scavenging activity was calculated.

$$\text{Antioxidant activity } (\%) = \frac{A_c - A_s}{A_c} \times 100 \quad (5)$$

where A_c is the absorbance of the control and A_s is the absorbance of the sample.

2.3.10. Attenuated total reflectance-Fourier transform infrared spectroscopy (ATR-FTIR). FTIR analysis of the films was performed using the transmittance mode (Bruker, Germany/Tensor II) in the 4000–400 cm^{-1} spectral region. The wavelength of the light absorbed, seen in the annotated spectrum, is a property of the chemical bonding.

2.3.11. Ultraviolet-visible spectroscopy. To verify the UV-barrier properties of the produced films, UV-vis spectroscopy data in the 230–800 nm range were obtained using a Tecan Systems Inc., San Jose, CA, USA TECAN Infinite® M200 pro-UV-vis spectrometer. Films were cut and inserted into cuvettes so there would be no space between the plate and the film. Every film reading was measured in triplicate. The empty cuvette was taken as a blank and measured. Eqn (6) below was then used to obtain the film's opacity value,

$$\text{Opacity value} = A_{600}/x \quad (6)$$

where "x" represents the thickness of the film and A_{600} indicates the absorption at 600 nm.

2.3.12. Thermal analysis. Differential scanning calorimetry (DSC) measurements were carried out between 30 °C and 200 °C using a DSC 25 system (TA Instruments). The first cooling and second heating curves were selected for analysis.

2.3.13. Overall migration studies. Overall migration of the extruded films was carried out as per European Union Regulation 10/2011.[24] The rectangular strips of each film sample were placed at two sides in contact with food simulants, like 3% acetic acid, 10% ethanol, 50% ethanol, and 90% ethanol in glass beakers. A lid-covered beaker was placed to prevent

Table 4 Mechanical properties of the PBAT/TKP blends[a]

Sample	Tensile strength	Young modulus (MPa)	EB (%)	Thickness (mm)
PT10	16.34 ± 0.93^d	388.54 ± 0.16^a	1594.41 ± 1.11^e	1.036 ± 0.005^a
PT20	9.32 ± 0.88^b	396.90 ± 0.10^b	850.88 ± 1.27^d	1.090 ± 0.001^b
PT30	9.15 ± 0.27^b	583.10 ± 0.30^d	666.56 ± 1.28^c	1.113 ± 0.005^c
PTG	11.11 ± 1.19^c	512.09 ± 0.13^c	647.03 ± 0.80^b	1.183 ± 0.005^d
PTP	7.48 ± 0.84^a	400.13 ± 0.69^b	642.46 ± 0.63^a	1.213 ± 0.005^e

[a] Each value is the standard deviation + the mean of the triplicates. As per Duncan's multiple range test, any two means in the same column that are separated by the same superscript letter were not substantially ($p > 0.05$) different.

© 2024 The Author(s). Published by the Royal Society of Chemistry

Open Access Article. Published on 18 settembre 2024. Downloaded on 05/04/2026 03:54:11.
This article is licensed under a Creative Commons Attribution-NonCommercial 3.0 Unported Licence.

Table 5 Water barrier properties of PBAT/TKP blends[a]

Sample	WVTR (g per m^2 per 24 h)	Water solubility (%)	Water absorption (%)
PT10	31.266 ± 0.029^a	0.0004 ± 0.0004^a	0.126 ± 0.115^a
PT20	41.281 ± 0.003^b	0.0007 ± 0.0002^{ab}	0.14 ± 0.017^a
PT30	50.706 ± 0.877^d	0.0021 ± 0.001^b	0.433 ± 0.128^b
PTG	47.473 ± 0.579^c	0.0057 ± 0.001^d	0.776 ± 0.231^c
PTP	58.582 ± 0.010^e	0.0041 ± 0.0008^c	0.573 ± 0.100^{bc}

[a] Each value is the standard deviation + the mean of the triplicates. According to Duncan's multiple range test, any two means in the same column that are separated by the same superscript letter were not substantially ($p > 0.05$) different.

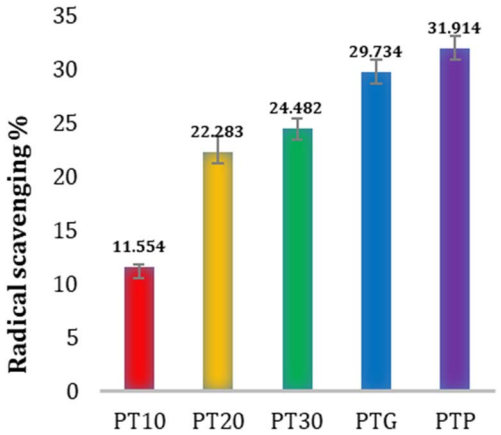

Fig. 1 Antioxidant properties of PBAT/TKP blends.

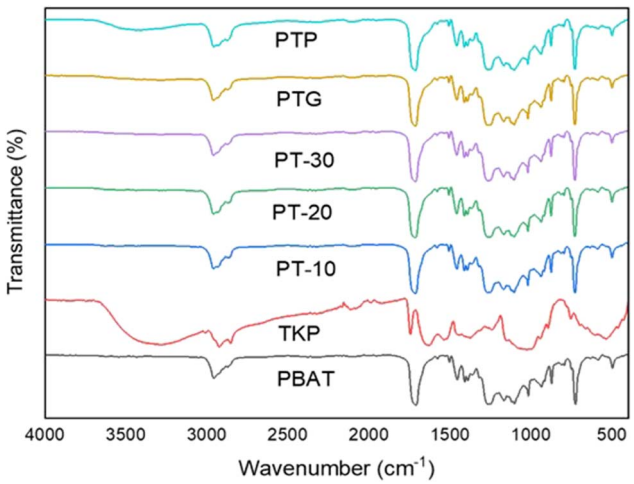

Fig. 2 FTIR of spectra of PBAT/TKP blends.

simulant evaporation during the contact period and this was placed in a thermostatically controlled chamber at 70 ± 0.5 °C for 2 h. The films were removed, and the simulant was placed in a pre-weighed dish and evaporated on a hotplate. The dishes containing the evaporation residue were kept in a thermostatically controlled oven at 105 ± 1.0 °C till completely dry, followed by 1 h in a desiccator, and then the weight was recorded. A balance capable of weighing up to 0.1 mg was used. The overall migration was calculated in mg dm^{-2}, where the exposed surface area of the test sample and the mg L^{-1} of the simulant were considered. Blank samples were run simultaneously, and each simulant's corrected migration values were calculated. For each plastic sample, triplicate measurements were performed, and the final migration value was the mean of the three values. Values were calculated using eqn (7)

$$\text{Migration value } (\text{mg dm}^{-2}) = \frac{\text{residual weight}}{\text{surface area}} \times 1000 \quad (7)$$

2.3.14. Biodegradability in soil. The methodology for evaluating the degradability of the films using the indoor soil burial method followed Amrutha *et al.* (2023) with a few changes.[25] Biodegradability was studied qualitatively since weight changes would be inaccurate due to the remaining dirt on the sample surface. Here, 15 cm of regional soil was applied to a pot maintained at room temperature (25 ± 2 °C) with a regulated relative humidity of 65 ± 5%. Initially, the materials were cut into 2 × 3 cm rectangular pieces and allowed to dry to remove any residual moisture. The films were then buried after being inserted inside a mesh support system. Watering was done daily to keep the soil wet. An evaluation was conducted by removing the films from the soil for 60 days, and images were recorded and saved to verify the samples visually.

2.3.15. Statistical analysis. Every film parameter was measured in triplicate for the film samples in repeated experiments. The results are provided as nominalization together with the standard deviation (SD). A one-way analysis of variance (ANOVA) was performed using the SPSS statistical analysis software for Windows (ver. 12.0, SPSS Inc., Chicago, IL, USA), and the significance of each mean property value was determined ($p < 0.05$) using Duncan's multiple range test.

3 Results and discussion

3.1. Physicochemical properties of tamarind kernel powder

Tamarind seed powder was determined for its physicochemical properties, and the results are tabulated in Table 2. As can be seen that the moisture and protein contents were around 6% and 18.70%, respectively. Similar results were reported by Akajiaku *et al.* (2014)[26] and Shalini P. *et al.* (2015).[27] The protein content of the tamarind seed has nutritional significance; hence, its intake will undoubtedly increase the total dietary intake of protein. Further, the fat content was 6.00 ± 0.34%, which was in accord with that reported by Yusuf *et al.* (2007)[12] of

Open Access Article. Published on 18 settembre 2024. Downloaded on 05/04/2026 03:54:11.
This article is licensed under a Creative Commons Attribution-NonCommercial 3.0 Unported Licence.

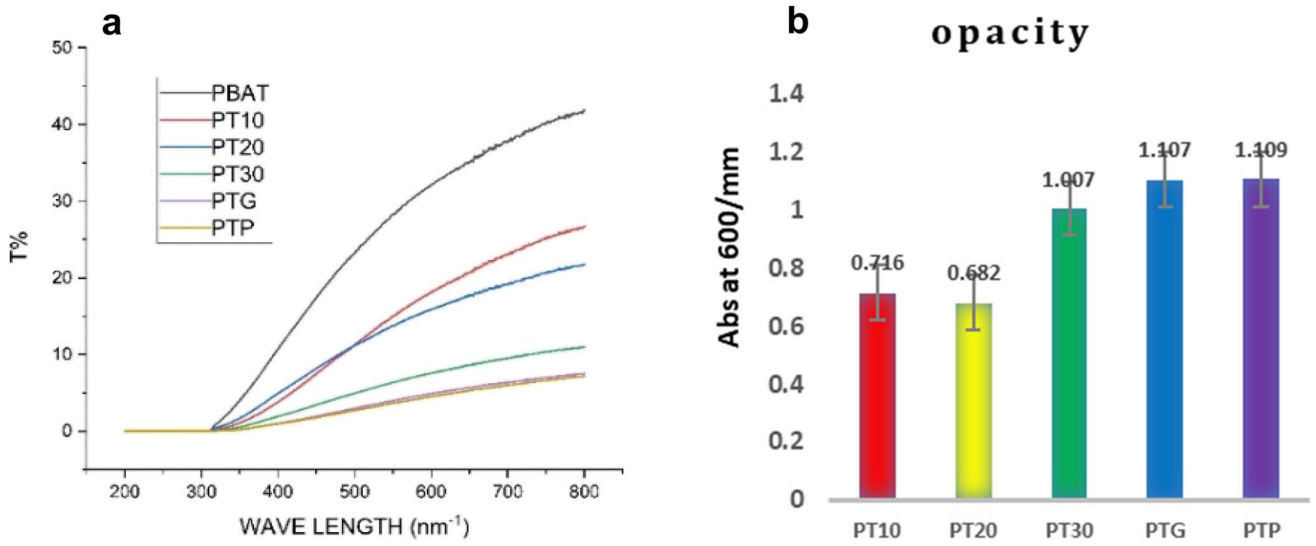

Fig. 3 Transmittance (a) and opacity (b) of PBAT/TKP blends.

6.94 ± 0.062%. The ash content and crude fiber content were found to be 3.79% and 0.49%, similar to those reported by Mahajani K. (2020).[28] Furthermore, the carbohydrates content, energy content, and hemicellulose xyloglucan were 71.14%, 368 kcal per 100 g, and 66.8% of total carbohydrates, correspondingly. The results obtained were the same as those reported in the literature by Johanis L. Y. *et al.* (2017)[29] (75.58% of carbohydrates) and T. Nguyen *et al.* (2019)[30] (64% of xyloglucan). The presence of low traces of non-starch components in TKP indicated that it had good purity. The parameters like the bulk density, tapped density, and Hausner's ratio refer to properties of the powder that enable better compressibility in different formulations. The results showed a bulk density of 0.38 g cm^3, 0.625 g cm^3 tap density, and a Hausner ratio of 1.625, which are

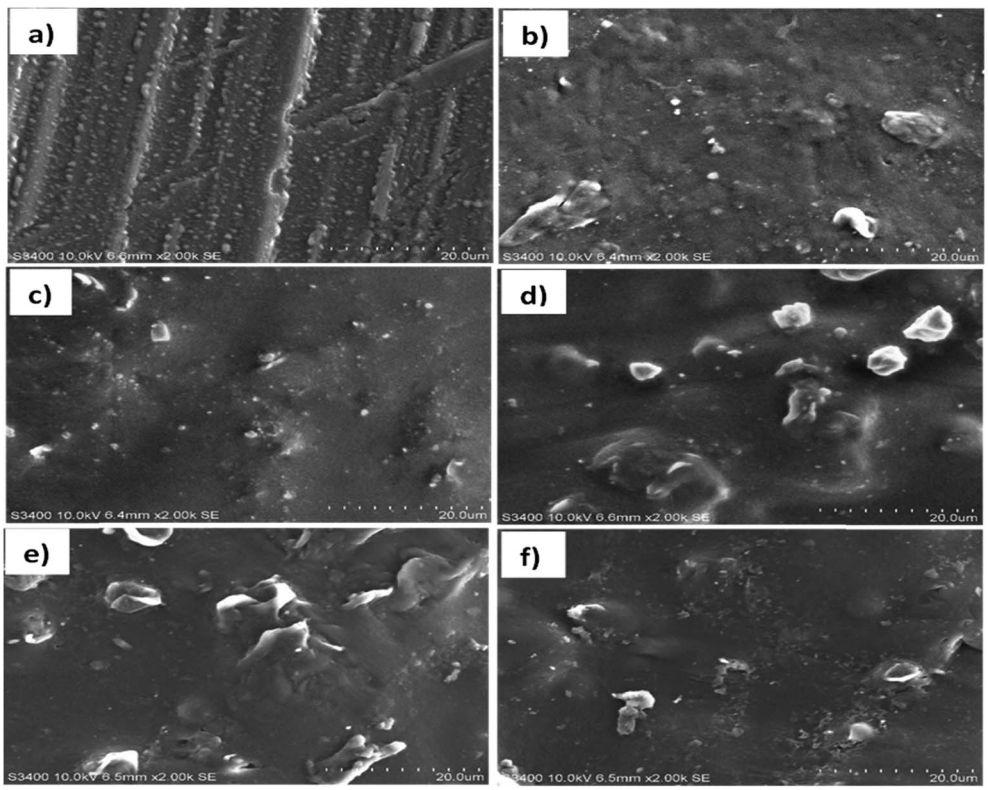

Fig. 4 SEM micrographs of PBAT/TKP blends: (a) PBAT, (b) PT-10, (c) PT-20, (d) PT-30, (e) PTG, and (f) PTP.

© 2024 The Author(s). Published by the Royal Society of Chemistry

Open Access Article. Published on 18 settembre 2024. Downloaded on 05/04/2026 03:54:11.
This article is licensed under a Creative Commons Attribution-NonCommercial 3.0 Unported Licence.

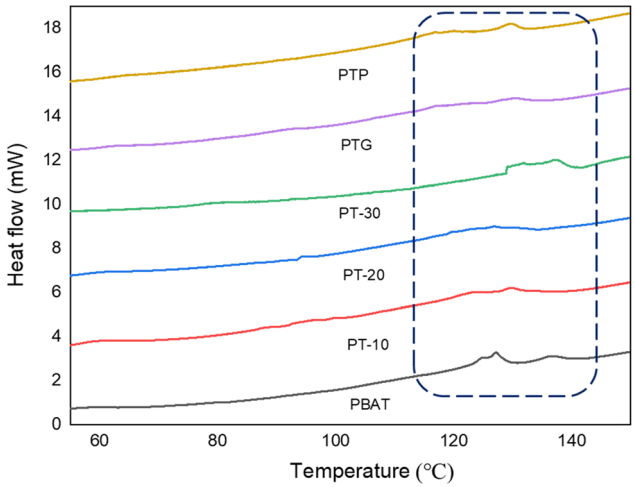

Fig. 5 DSC of PBAT and PBAT/TKP blends.

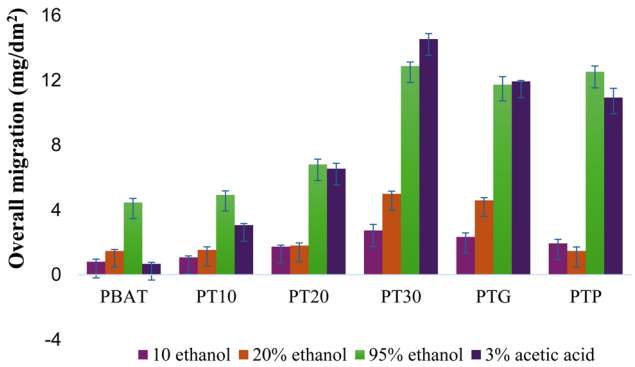

Fig. 6 Overall migration of PBAT/TKP blends.

closer to the reported findings of Saikia *et al.* (2017).[31] The values were found to be within the limits, indicating potentially good flow properties and compressibility. Other properties, such as the angle of repose of 34.85°, viscosity of 512 cP (1% solution of TKP), highest WAI of 415.375 ± 1.39%, and WSI of 38.784 ± 1.14% were observed.

3.2. Melt flow index

The rate at which a polymer melt flows under pressure and temperature is represented by the melt flow index (MFI), an important metric that indirectly determines the viscosity of the melt. The MFI values of the PBAT/TPK blends are shown in Table 3. Commercial grade PBAT possessed an MFI of around 5 g/10 min, indicating that it is highly viscose in nature due to its high molecular weight. With the addition of 10 wt% TKP, MFI increased to 17 g/10 min, whereas with further addition of up to 30 wt%, the MFI decreased to 11.75 g/10 min. This could be accredited to the more TKP in the matrices, which increased the viscosity and resulted in less flow. Thus, the aggregation of TKP particles was seen at 30 wt%, while a uniform dispersion was observed at 10 wt%. Further, after incorporating plasticizers into the blends, MFI was still reduced to 7 g/10 min due to the lubrication effect of the plasticizers and improved dispersion of TKP in the PBAT matrix. Conversely, the viscosity was increased compared to blends without plasticizers.[32]

3.3. Mechanical properties

The mechanical parameters, including thickness, Young's modulus (YM), elongation at break (EB), and tensile strength (TS), are presented in Table 4. These attributes are affected by the homogeneity of the film matrices. Considering the tensile properties, the PT10 film showed a tensile strength of 16 MPa, EB of 1594%, and Young's modulus of 367 MPa. Increasing concentrations of TKP resulted in decreased TS and EB values. This might be due to the discontinuity of the PBAT matrix resulting from TKP network interruption, which reduces the cohesion between PBAT molecules, while the MFI was found to be reduced for the highest concentration of TKP, consequently reducing the elongation. Increased stiffness was also observed, which might be assigned to the inherent rigidity of TKP according to Chaiwutthinan P. *et al.* (2019).[33] In the case of formulations with plasticizers, PTP showed the lowest tensile properties compared to the glycerol-based blend. This was probably due to bulky groups of PEG-induced voids that restricted the transfer of applied load, resulting in an easy breakage of the material.[34] The thickness of the film increased with increasing the TKP ratio because of the uneven dispersion of starch in the matrix. It could be concluded that the stiffness of PBAT was improved by the addition of TKP.

3.4. Water barrier properties

Water vapor permeability can negatively affect the shelf life of packaged foods. Hence, the WVTR is an important parameter to determine.[35] The WTVR results are presented in Table 5. Since pure PBAT is hydrophobic, it had a WVTR of 24.28 g per m^2 per day. As expected, the inclusion of TKP into PBAT increased the transmission rate due to the inherent hydrophilic nature of TKP, which was due to the presence of more hydroxyl groups within it. The higher the TKP ratio, the greater the reduction in barrier property, because the poor interfacial adhesion of TKP in the matrix resulted in the formation of voids, which further decreased the tortuous path. It is important to note that formulations based on glycerol showed the least barrier toward moisture. However, the PEG-added blends exhibited much less transmission than glycerol, attributed to the good dispersion of TKP in PBAT probably reducing the voids. Overall, it is important to find a promising method to improve the barrier properties of PBAT/TKP blends as these formulations do not currently have the potential to be used in primary packaging.[36,37] Higher concentrations of TKP in the blend can provide more sites for water molecules to interact. It was found there that as the TKP concentration increased, more hydroxyl molecules were available for dissolution in water, leading to a higher water solubility index.

3.5. Antioxidant property

Packaging films with antioxidant activity can improve the shelf life of packaged food. Using the DPPH radical scavenging assay,

Open Access Article. Published on 18 settembre 2024. Downloaded on 05/04/2026 03:54:11.
This article is licensed under a Creative Commons Attribution-NonCommercial 3.0 Unported Licence.

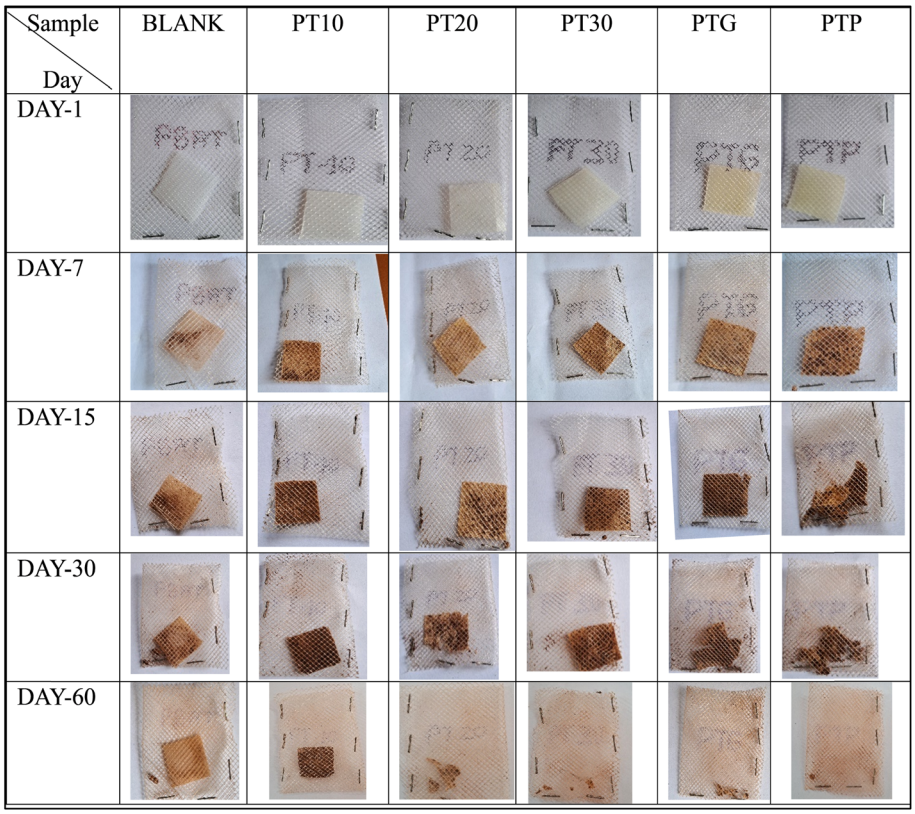

Fig. 7 Biodegradation studies of PBAT/TKP blends.

the antioxidant activity of the produced films was assessed and the results are displayed in Fig. 1. A remarkable radical scavenging activity was noticed in the PBAT/TKP-based films. This could be attributed to the inherent presence of bioactive compounds in TKP, which helped in radical scavenging.[38] Further, the plasticizers-based films also showed activity because glycerol and PEG have antioxidant ability. Thus, it can be inferred that the PTP blend films exhibited the highest antioxidant activity due to the synergistic effect of PEG and TKP. PBAT/TKP can also be used as antioxidant packaging for foods prone to oxidative degradation.[39]

3.6. FTIR analysis

The surface functional group characteristic of PBAT/TKP composites is displayed in Fig. 2. The characteristic peak at 2957 cm^{-1} corresponded to the asymmetric stretching of CH_2 in PBAT. The PBAT/TKP blend films exhibited a broad peak at around 3350–3400 cm^{-1}, which was attributed to –OH stretching vibration due to the substantial number of hydroxyl groups in TKP.[40] For PBAT, the bending vibration of the –CH plane of the benzene ring was associated with a peak at 725 cm^{-1}; the *trans*-C–O symmetric stretching vibration was found to be associated with a peak at 937 cm^{-1}; the bending vibration at the surface of adjacent hydrogen atoms on the phenyl ring was associated with a peak at 1018 cm^{-1}; the left-right symmetric stretching vibration of C–O was identified as the source of the peak at 1103 cm^{-1}; the C–O symmetric stretching vibration was associated with a peak at 1265 cm^{-1}; the *trans*-CH_2– plane bending vibration was associated with a peak at 1408 cm^{-1}; the skeletal vibration of the benzene ring was associated with a peak at 1504 cm^{-1}, the C–O stretching vibration was linked to a peak at 1713 cm^{-1}, and the CH_2 asymmetric stretching vibration was linked to a peak at 2959 cm^{-1}.[41] The intensity of the peaks at 2957 cm^{-1} was increased for PTP compared to the other blends, confirming the excellent interaction between PBAT, TKP, and PEG.

3.7. UV spectroscopy

The UV-visible light transmittance of the PBAT/TKP composite films was measured to further explore these films' transparency, as depicted in Fig. 3. The PBAT/TKP blends exhibited a lower UV transmittance compared to neat PBAT. The transmittance of the PBAT/TKP composite films with plasticizers was even less. A polymeric film's light transmittance depends on the shape of the film in addition to its chemical structure and molar mass.[42] The morphology of the films was affected by the presence of TKP. TKP particles that were not fully molten during the extrusion were responsible for light refraction. PTG and PTP exhibited even lower transmittance readings in the visible-light region, likely due to the higher TKP concentration, which was not gelatinized, as observed in the micrographs. The decline in transmittance was attributed to the light impenetrability in the

© 2024 The Author(s). Published by the Royal Society of Chemistry

Open Access Article. Published on 18 settembre 2024. Downloaded on 05/04/2026 03:54:11.
This article is licensed under a Creative Commons Attribution-NonCommercial 3.0 Unported Licence.

PBAT/TKP matrix. In other words, the UV-absorption capacity of the blends indicated an effective UV-barrier property in the prepared films. This barrier property might inhibit the packaged product's quality deterioration, as well as lipid oxidation, color change, and off-flavor formation, usually provoked by UV–food interactions. Further, the opacity was found to be increased with the increase in the concentration of TKP powder; whereby, the film's color turned dark creamish, thus showing higher opacity.

3.8. Scanning electronic microscopy

The film's surface morphology is displayed in Fig. 4. The pure PBAT film (Fig. 4a) showed a uniform surface without any disturbances, since PBAT was only a continuous phase. The blending of TKP into the PBAT matrix (Fig. 4b and c) produced discrepancies because of the incomplete melting of TKP and the incompatibility between the hydrophilic tamarind kernel powder and hydrophobic PBAT.[43,44] Fig. 4d shows the SEM of the PBAT blend with 30 wt% TKP, where a more co-continuous phase could be observed due to the higher content of TKP, resulting in more connected granules. Further, the incorporation of plasticizers improved the phase morphology. This was ascertained because the lubrication effect of the plasticizers increased the dispersion of TKP, thereby forming smoother surface films. The glycerol and PEG-added films (Fig. 4e and f) showed better plasticization than the former case. It can be observed that the PEG improved interfacial interaction between PBAT and TKP due to its high molecular weight.[45,46] Hence, it could be concluded that the PTP blend films exhibited better surfaces compared to all the other formulations.

3.9. Thermal analysis

DSC analysis of the PBAT/TKP blends revealed only melting peaks between 127–129 °C, as could be observed in Fig. 5. The pure PBAT film exhibited an intensified melting peak at 127 °C. The addition of tamarind kernel powder into PBAT widened the melting peaks, which could be attributed to tamarind kernel powder disturbing the uniform chain segments of the PBAT matrix, which could be seen in the SEM micrographs.[47] In addition, a slight upshift of the melting temperature could be observed with increasing the TKP concentration, which might have resulted from the interaction between the blend matrices.[48] Regarding the plasticizers-added blends, the glycerol-incorporated films showed almost indiscernible melting peaks due to the plasticizing effect inducing a free volume in the matrix, whereas a pronounced peak could be noticed in the PEG mixed blends due to its compatibilizing effect, resulting in good interactions between the matrices.

3.10. Migration analysis

Migration analysis was carried out with different simulants, like 3% acetic acid, 10% ethanol, 50% ethanol, and 90% ethanol, using gravimetric analysis as per European standards 10/2011 and the results are presented in Fig. 6. The standard limit for the migration range was less than 10 mg dm^{-2}. The overall migration values for the pure PBAT films were less than 10 mg dm^{-2}. The migration values of the PBAT films were due to the non-volatile organic compounds.[49] On the other hand, it was apparent that there was a higher migration for PBAT/TKP blend films as the powder was not fully adhered to the PBAT matrix and was unsuitable for liquids. Hence, it can be concluded that these packaging films should be used for direct contact only with solid and dry food matrices, like fruits and vegetables. However, they could also be used for secondary and tertiary foods, and other non-food applications, like carry bags and agricultural mulch films.

3.11. Biodegradability studies of the PBAT/TKP films

Evaluating biodegradability is critical to understanding the interaction of developed films with the environment and the time required for their degradation. The soil burial test is practical and gives a picture of biodegradation. In the present study, degradation studies were performed qualitatively to observe the changes in the film's area, as shown in Fig. 7. As expected, the 30% TKP blend with and without plasticizer demonstrated rapid degradation compared to the other films. Because of the hydrophilic natures of TKP, glycerol, and PEG, the hydrolytic activity in the polymer matrix destabilizes the intermolecular interaction, favoring microbes' growth, and it ultimately disintegrates.[50] This study was carried out for 60 days. All the films were biodegradable except pure PBAT and PT10. These films' biodegradability could be altered as per requirements, which is a substantial finding for their use in food packaging or other industries.

4 Conclusion

In this work, the effects of glycerol and polyethylene glycol as plasticizers on the mechanical properties, water absorption, morphology, and overall migration of PBAT/TPS blends with different ratios of PBAT and TKP were investigated. The mechanical properties were affected by the structure of the plasticizer. At a 30% content of TKP, the tensile strength and elongation at break were the highest in the presence of glycerol. The opacity was found to be increased with the increasing concentration of TKP powder. The UV transmittance of the PBAT/TKP blends was lower than for the neat PBAT. The reduction in transmittance was attributed to the light impenetrability into the PBAT/TKP matrix, which can impart an effective UV-barrier property to the films. PEG improved the interfacial interaction between PBAT and TKP and PTP, and the blend films exhibited a better surface than all other formulations, according to the morphological studies. The biodegradation rate was increased for higher concentrations of TKP with PEG films. Overall, the migration studies showed that these developed films could be used for secondary, tertiary food, and other non-food applications, like carry bags and mulch films. Therefore, blending TKP and bioplastics enhances the overall attributes of the plastic along with being cost-effective and contributing to sustainability. Further, potential applications of TKP-based bioplastics for agricultural mulching film applications should be evaluated.

Open Access Article. Published on 18 settembre 2024. Downloaded on 05/04/2026 03:54:11.
This article is licensed under a Creative Commons Attribution-NonCommercial 3.0 Unported Licence.

Data availability

The supporting data in the study will be provided by the corresponding author upon the appropriate request.

Author contributions

Rokalla Preethi: investigation; data curation; methodology; formal analysis; original draft writing-review and editing. NR Amrutha: methodology, validation, review, and editing. Keshava Murthy PS: resources and validation. Jeevan Prasad Reddy: conceptualization, supervision, review, and editing.

Conflicts of interest

The authors declare that they have no conflict of interest.

Acknowledgements

The authors are greatly acknowledged the University Grants Commission (UGC)(Ref. No. 20051013458) for funding this research. We also acknowledge the Academy of Scientific and Innovative Research (AcSIR), Ghaziabad, and CSIR-CFTRI, Mysore, India, for their kind support.

References

1 S. Roy, T. Ghosh, W. Zhang and J. W. Rhim, Recent progress in PBAT-based films and food packaging applications: a mini-review, *Food Chem.*, 2024, **437**, 137822, DOI: 10.1016/j.foodchem.2023.137822.
2 Market, retrieved from https://www.european-bioplastics.org/market/, accessed 30 September 2020.
3 S. Shaikh, M. Yaqoob and P. Aggarwal, An overview of biodegradable packaging in the food industry, *Curr. Res. Food Sci.*, 2021, **4**, 503–520, DOI: 10.1016/j.crfs.2021.07.005.
4 S. Mangaraj, A. Yadav, L. M. Bal, S. K. Dash and N. K. Mahanti, Application of biodegradable polymers in food packaging industry: a comprehensive review, *J. Packag. Technol. Res.*, 2019, **3**, 77–96, DOI: 10.1007/s41783-018-0049-y.
5 J. Kadzińska, M. Janowicz, S. Kalisz, J. Bryś and A. Lenart, An overview of fruit and vegetable edible packaging materials, *Packag. Technol. Sci.*, 2019, **32**(10), 483–495, DOI: 10.1002/pts.2440.
6 C. V. Dhumal, J. Ahmed, N. Bandara and P. Sarkar, Improvement of antimicrobial activity of sago starch/guar gum bi-phasic edible films by incorporating carvacrol and citral, *Food Packag. Shelf Life*, 2019, **21**, 100380, DOI: 10.1016/j.fpsl.2019.100380.
7 P. Goyal, V. Kumar and P. Sharma, Carboxymethylation of tamarind kernel powder, *Carbohydr. Polym.*, 2007, **69**(2), 251–255, DOI: 10.1016/j.carbpol.2006.10.001.
8 S. Jana, K. K. Sen and S. K. Basu, In vitro aceclofenac release from IPN matrix tablets composed of chitosan-tamarind seed polysaccharide, *Int. J. Biol. Macromol.*, 2014, **65**, 241–245, DOI: 10.1016/j.fpsl.2019.100380.
9 C. Rodrigues, J. M. de Mello, F. Dalcanton, D. L. Macuvele, N. Padoin, M. A. Fiori, C. Soares and H. G. Riella, Mechanical, thermal and antimicrobial properties of chitosan-based-nanocomposite with potential applications for food packaging, *J. Polym. Environ.*, 2020, **28**, 1216–1236, DOI: 10.1007/s10924-020-01678-y.
10 I. Yadav, S. K. Nayak, V. S. Rathnam, I. Banerjee, S. S. Ray, A. Anis and K. Pal, Reinforcing effect of graphene oxide reinforcement on the properties of poly (vinyl alcohol) and carboxymethyl tamarind gum based phase-separated film, *J. Mech. Behav. Biomed. Mater.*, 2018, **8**, 61–71, DOI: 10.1016/j.jmbbm.2018.02.021.
11 R. Santhosh, M. Hoque, I. Syed and P. Sarkar, Polysaccharide–oil Complexes as Edible Films, *Food, Medical, and Environmental Applications of Polysaccharides*, Elsevier, 2021, pp. 109–133, DOI: 10.1016/B978-0-12-819239-9.00014-2.
12 A. A. Yusuf, B. M. Mofio and A. B. Ahmed, Proximate and mineral composition of Tamarindus indica Linn 1753 seeds, *Sci. World*, 2007, **2**(1), 1–4, DOI: 10.4314/swj.v2i1.51699.
13 Y. X. Weng, Y. J. Jin, Q. Y. Meng, L. Wang, M. Zhang and Y. Z. Wang, Biodegradation behavior of poly (butylene adipate-co-terephthalate)(PBAT), poly (lactic acid)(PLA), and their blend under soil conditions, *Polym. Test.*, 2013, **32**(5), 918–926, DOI: 10.1016/j.polymertesting.2013.05.001.
14 I. Vroman and L. Tighzert, Biodegradable polymers, *Materials*, 2009, **2**(2), 307–344, DOI: 10.3390/ma2020307.
15 F. V. Ferreira, L. S. Cividanes, R. F. Gouveia and L. M. Lona, An overview on properties and applications of poly (butylene adipate-co-terephthalate)–PBAT based composites, *Polym. Eng. Sci.*, 2019, **59**, 7–15, DOI: 10.1002/pen.24770.
16 R. Herrera, L. Franco, A. Rodríguez-Galán and J. Puiggalí, Characterization and degradation behavior of poly (butylene adipate-co-terephthalate), *J. Polym. Sci., Part A: Polym. Chem.*, 2002, **40**(23), 4141–4157, DOI: 10.1002/pola.10501.
17 F. Ivanič, M. Kováčová and I. Chodák, The effect of plasticizer selection on properties of blends poly (butylene adipate-co-terephthalate) with thermoplastic starch, *Eur. Polym. J.*, 2019, **116**, 99–105, DOI: 10.1016/j.eurpolymj.2019.03.042.
18 T. M. Shivani and M. A. Sathiavelu, Comprehensive review on functionality of probiotics in edible packaging, *Packag. Technol. Sci.*, 2023, **36**(1), 15–30, DOI: 10.1002/pts.2690.
19 AOAC, *Official Methods of Analysis*, Association of Official Analytical Chemists, Washington, DC, 15th edn, 2000.
20 ASTM D1238-2023, *Standard test method for melt flow rate of thermoplastics by extrusion plastometer*, American Society for Testing and Materials, 2023.
21 ASTM D882-02, *Standard test methods for tensile properties of thin plastic sheeting*, American Society for Testing and Material, 2002.
22 ASTM E96-00, *Standard test methods for water vapor transmission of materials*, American Society for Testing and Material, 1996.

© 2024 The Author(s). Published by the Royal Society of Chemistry

Open Access Article. Published on 18 settembre 2024. Downloaded on 05/04/2026 03:54:11.
This article is licensed under a Creative Commons Attribution-NonCommercial 3.0 Unported Licence.

23 ASTM D570, *Standard Test Method for Water Absorption of Plastics*, American Society for Testing and Material, 2022.
24 European commission – food contact materials, retrieved from **https://food.ec.europa.eu/safety/chemical-safety/food-contact-materials_en**.
25 N. R. Amrutha, M. A. Dhale, A. Job, K. Divyalakshmi, D. J. P. Reddy and P. S. K. Murthy, Silver Nanoparticles Incorporated PVA-MC Blends: A Systematic Approach to Understand its Properties for Food Packaging Applications, *ChemistrySelect*, 2023, **8**(27), e202205031, DOI: **10.1002/slct.202205031**.
26 L. O. Akajiaku, J. N. Nwosu, N. C. Onuegbu, N. E. Njoku and C. O. Egbeneke, Proximate, mineral and anti-nutrient composition of processed (soaked and roasted) Tamarind (Tamarindus indica) seed nut, *Curr. Res. Nutr. Food Sci.*, 2014, **2**(3), 136–145, DOI: **10.12944/CRNFSJ.2.3.05**.
27 P. Shalini and K. R. S. Murthy, Proximate composition, antinutritional factors and protein fractions of Tamarindus indica L. seeds as influenced by processing treatments, *Int. J. Food Nutr. Sci.*, 2015, **4**(4), 91–96.
28 K. Mahajani, Physicochemical, functional properties and proximate composition of tamarind seed: proximate composition of tamarind seed, *Journal of AgriSearch*, 2020, **7**(1), 51–53, DOI: **10.21921/jas.v7i01.17636**.
29 L. Y. Johanis, O. Sjofjan, I. H. Djunaidi and S. Suyadi, Effect of processing methods on nutrient and tannin content of tamarind seeds, *Intl. J. Trop. Drylands*, 2017, **1**(2), 78–82, DOI: **10.13057/tropdrylands/t010203**.
30 T. T. Nguyen, W. Jittanit and W. Srichamnong, Production of xyloglucan component extracted from tamarind (Tamarindus indica) seeds using microwave treatment for seed decortication, *J. Food Process. Preserv.*, 2019, **43**(8), e14055, DOI: **10.1111/jfpp.14055**.
31 F. Saikia, J. O. Ali and B. I. Das, Isolation and characterization of tamarind seed polysaccharides—a natural release retardant, *Int. J. Curr. Pharm. Res.*, 2017, **9**, 114–117, DOI: **10.22159/ijcpr.2017v9i4.20972**.
32 H. F. Giles Jr, J. R. Wagner Jr and E. M. Mount III, Extrusion Process, *Extrusion*, Norwich, NY, 2005, pp. 1–8.
33 P. Chaiwutthinan, S. Chuayjuljit, S. Srasomsub and A. Boonmahitthisud, Composites of poly (lactic acid)/poly (butylene adipate-co-terephthalate) blend with wood fiber and wollastonite: physical properties, morphology, and biodegradability, *J. Appl. Polym. Sci.*, 2019, **136**(21), 47543, DOI: **10.1002/app.47543**.
34 F. P. La Mantia, M. Ceraulo, M. C. Mistretta and M. Morreale, Effect of cold drawing on mechanical properties of biodegradable fibers, *J. Appl. Biomater. Funct. Mater.*, 2017, **15**(1), 70–76, DOI: **10.5301/jabfm.5000328**.
35 S. Roy, S. J. Min, D. Biswas and J. W. Rhim, Pullulan/chitosan-based functional film incorporated with curcumin-integrated chitosan nanoparticles, *Colloids Surf., A*, 2023, **660**, 130898, DOI: **10.1016/j.matdes.2024.113080**.
36 C. C. Chang, B. M. Trinh and T. M. Mekonnen, Robust multiphase and multilayer starch/polymer (TPS/PBAT) film with simultaneous oxygen/moisture barrier properties, *J. Colloid Interface Sci.*, 2021, **593**, 290–303, DOI: **10.1016/j.jcis.2021.03.010**.
37 W. Zhang, S. Roy and J. W. Rhim, Copper-based nanoparticles for biopolymer-based functional films in food packaging applications, *Compr. Rev. Food Sci. Food Saf.*, 2023, **22**(3), 1933–1952, DOI: **10.1111/1541-4337.13136**.
38 H. S. Lopes, G. H. Oliveira, S. I. Talabi and A. A. Lucas, Production of thermoplastic starch and poly (butylene adipate-co-terephthalate) films assisted by solid-state shear pulverization, *Carbohydr. Polym.*, 2021, **258**, 117732, DOI: **10.1016/j.carbpol.2021.117732**.
39 N. Limsangouan, N. Milasing, M. Thongngam, P. Khuwijitjaru and W. Jittanit, Physical and chemical properties, antioxidant capacity, and total phenolic content of xyloglucan component in tamarind (Tamarindus indica) seed extracted using subcritical water, *J. Food Process. Preserv.*, 2019, **43**(10), e14146, DOI: **10.1111/jfpp.14146**.
40 S. Roy and J. W. Rhim, Curcumin incorporated poly (butylene adipate-co-terephthalate) film with improved water vapor barrier and antioxidant properties, *Materials*, 2020, **13**(19), 4369, DOI: **10.3390/ma13194369**.
41 N. Bumbudsanpharoke, N. Harnkarnsujarit, B. Chongcharoenyanon, S. Kwon and S. Ko, Enhanced properties of PBAT/TPS biopolymer blend with CuO nanoparticles for promising active packaging, *Food Packag. Shelf Life*, 2023, **37**, 101072, DOI: **10.1016/j.fpsl.2023.101072**.
42 E. C. Cardoso, D. F. Parra, S. R. Scagliusi, R. M. Sales, F. Caviquioli and A. B. Lugão, Study of bio-based foams prepared from PBAT/PLA reinforced with bio-calcium carbonate and compatibilized with gamma radiation, *Use Gamma Radiat. Tech. Peaceful Appl. Intech Open*, 2019, **139**, 1, DOI: **10.5772/intechopen.85462**.
43 X. Jiang, J. Wang, J. Zhang, J. Wang and W. Guo, Preparation of high-performance poly (butylene adipate-co-terephthalate)/thermoplastic starch compounds with epoxidized soybean oil as compatibilizer, *Polym. Eng. Sci.*, 2023, **63**(9), 2878–2890, DOI: **10.1002/pen.26412**.
44 T. Panrong, T. Karbowiak and N. Harnkarnsujarit, Effects of acetylated and octenyl-succinated starch on properties and release of green tea compounded starch/LLDPE blend films, *J. Food Eng.*, 2020, **284**, 110057, DOI: **10.1016/j.jfoodeng.2020.110057**.
45 M. Dammak, Y. Fourati, Q. Tarrés, M. Delgado-Aguilar, P. Mutjé and S. Boufi, Blends of PBAT with plasticized starch for packaging applications: mechanical properties, rheological behaviour and biodegradability, *Ind. Crops Prod.*, 2020, **144**, 112061, DOI: **10.1016/j.indcrop.2019.112061**.
46 R. P. Brandelero, M. V. Grossmann and F. Yamashita, Effect of the method of production of the blends on mechanical and structural properties of biodegradable starch films produced by blown extrusion, *Carbohydr. Polym.*, 2011, **86**(3), 1344–1350, DOI: **10.1016/j.carbpol.2011.06.045**.
47 J. Nagarjun, J. Kanchana, G. R. Kumar, S. Manimaran and M. Krishnaprakash, Enhancement of mechanical behavior of PLA matrix using tamarind and date seed micro fillers,

Open Access Article. Published on 18 settembre 2024. Downloaded on 05/04/2026 03:54:11.
This article is licensed under a Creative Commons Attribution-NonCommercial 3.0 Unported Licence.

J. Nat. Fibers, 2022, **19**(12), 4662–4674, DOI: **10.1080/15440478.2020.1870616**.

48 S. Mohanty and S. K. Nayak, Starch based biodegradable PBAT nanocomposites: effect of starch modification on mechanical, thermal, morphological and biodegradability behavior, *Int. J. Plast. Technol.*, 2009, **13**(2), 163–185, DOI: **10.1007/s12588-009-0013-3**.

49 J. Lin, W. L. Wu, A. H. Zhong, Y. P. Xian, H. N. Zhong, B. Dong, M. Liang, J. P. Hu, Y. N. Wu, X. F. Yang and H. X. Sui, Non-targeted analysis and risk assessment of intentionally and non-intentionally added substances migrating from the emerging biodegradable food contact material poly (butylene adipate-co-terephthalate)/modified starch blend film, *Food Packag. Shelf Life*, 2023, **40**, 101190, DOI: **10.1016/j.fpsl.2023.101190**.

50 C. G. Vargas, T. M. Costa, A. de Oliveira Rios and S. H. Flôres, Comparative study on the properties of films based on red rice (Oryza glaberrima) flour and starch, *Food Hydrocolloids*, 2017, **65**, 96–106, DOI: **10.1016/j.foodhyd.2016.11.006**.

© 2024 The Author(s). Published by the Royal Society of Chemistry